On-board voltage regulation for all-electric DC ships

Haseltalab, Ali; Botto, Miguel Ayala; Negenborn, Rudy R.

DOI
10.1016/j.ifacol.2018.09.500

Publication date
2018

Document Version
Final published version

Published in
IFAC-PapersOnLine

Available online at www.sciencedirect.com

ScienceDirect

IFAC Papers Online CONFERENCE PAPER ARCHIVE

IFAC PapersOnLine 51-29 (2018) 341–347

On-Board Voltage Regulation For All-Electric DC Ships ⋆

Ali Haseltalab *, **Miguel Ayala Botto** **, **Rudy R. Negenborn** *

* *Department of Maritime and Transport Technology, Delft University of Technology, Delft, the Netherlands (e-mail: {a.haseltalab,r.r.negenborn}@ tudelft.nl).*

** *LAETA, IDMEC, Instituto Superior Técnico, Universidade de Lisboa, Portugal (e-mail: ayalabotto@tecnico.ulisboa.pt)*

Abstract: In this paper, a control strategy is proposed for the voltage regulation and the shaft speed control of diesel generators on-board of all-electric ships with Direct Current (DC) power and propulsion systems. The proposed methodology is based on Input-Output Feedback Linearization (IOFL) of the prime mover dynamical model. First, a model for different components in the system is represented and by merging them, the overall model of the system is obtained in state space format. Then, an IOFL-based control algorithm is applied for stabilization, voltage regulation and shaft speed control of the diesel generator. The performance of the algorithm is assessed using a model of an inland vessel.

Keywords: On-Board DC Power System, Voltage Regulation, Input-Output Feedback Linearization, Diesel Generator-Rectifier.

1. INTRODUCTION

Due to the international pressure on shipping industry to reduce its emissions and increase efficiency, the industry is moving toward more green solutions (Geertsma et al. (2017)). As a result of this push, and also for accommodating the ever-increasing different power demands efficiently, the adoption of all-electric configurations for the on-board power and propulsion system has become a popular trend. In such configurations, the chemical energy of the fuel is translated into electrical energy by the use of diesel generators and then converted to mechanical energy through induction motors that are connected to the propellers. With the recent advances in the field of semiconductors, DC microgrids are considered as a potential solution for energy conservation problems in the shipping industry with which the flexibility in design and weight saving is increased (Zahedi and Norum (2013)) and in addition, the number of converting stages in ships is decreased.

However, still, there exist several issues with the deployment of DC power and propulsion systems related to system stability and robustness, as well as the lack of feasible fault-detection and isolation strategies. The strive to address stability issues is increasing both in academia and industry. In Zahedi and Norum (2013), for the main components in a power and propulsion system a model is given and based on these models the overall system is modeled and simulated. In Zhu et al. (2018), a simplified model for the overall system is presented and by adoption of controllable rectifiers, an algorithm is presented to regulate the DC voltage. In Helland (2015), the stability of the DC voltage is analyzed where diode-bridge rectifiers are coupled with synchronous generators. Modeling and simulation of the same system with addition of a battery-converter set are carried out in Syverud (2016) where conventional techniques are used for the voltage regulation. In Zadeh et al. (2013), a methodology is proposed to stabilize the DC voltage by moving the states of the system into a previously found region of attraction. A semidefinite programming-based control algorithm is presented in Herrera et al. (2017) which is accompanied by an stability analysis of DC microgrids under constant loads. The robustness and performance of the on-board power system is also dependent on power and energy management methodologies. In Haseltalab and Negenborn (2017), after modeling a DC on-board power and propulsion system, a power management algorithm is presented to increase the efficiency of the on-board power system and boost the stability of the system by prohibiting enormous changes in the delivered power by each Diesel Generator Rectifier (DGR) set. In the literature, there are several methodologies to address the stability issues within DC microgrids by adoption of distributed control techniques where the focus was mainly on the droop control (Farasat et al. (2015), Li et al. (2014)). For more information regarding control of DC grids the reader is referred to Meng et al. (2017).

Taking into account, the stability issues within the on-board DC microgrids, and also insufficiency of linear methods for voltage regulation and shaft speed control of diesel generators (Meng et al. (2017)), an algorithm is proposed which can be a potential replacement for linear conventional methods for DC voltage-regulation and shaft speed

⋆ This research is supported by the project ShipDrive: A Novel Methodology for Integrated Modelling, Control, and Optimization of Hybrid Ship Systems (project 13276) of the Netherlands Organisation for Scientific Research (NWO), domain Applied and Engineering Sciences (TTW).

10.1016/j.ifacol.2018.09.500

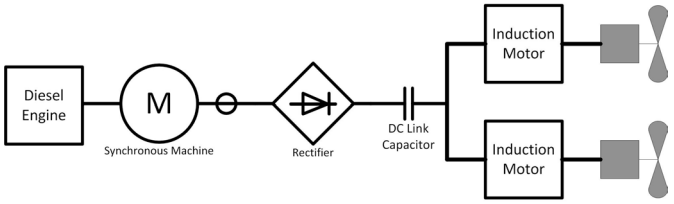

Fig. 1. Power and Propulsion system under study.

control of diesel generators under varying loads. Prior to the presentation of the algorithm, the modeling of the system is carried out where a model for each component is first presented. Then, by a suitable choice of the state variables, the overall state-space model is obtained by merging all model components. In the context of this paper, six-pulse uncontrollable rectifiers are considered for the AC to DC conversion which are cheaper and require less space and lower maintenance effort. The proposed voltage and diesel generator shaft speed control methodology is based on Input-Output Feedback Linearization (IOFL) where the model of the overall system is taken into account for the control purposes. By implementing this IOFL rule, the system behaves like a linear system. Later, in order to evaluate the performance of our proposed methodology, the algorithm is applied to a model we previously developed in Haseltalab and Negenborn (2017) for all-electric ships with DC power and propulsion systems.

The rest of the paper is organized as follows. In Section 2, a mathematical model for every component is given and the overall system model is formulated in state-space format. In Section 3, the IOFL-based control algorithm is presented. The evaluation of the proposed strategy is carried out in Section 4 where the algorithm is applied to a Diesel Generator Rectifier (DGR) set on-board of an inland cargo vessel. In Section 5, conclusions and future research directions are given.

2. SYSTEM DESCRIPTION

In this section the overall system is described and modeled using dynamical equations in state space format.

On-board DC microgrids consist of prime-mover(s), AC/DC conversion modules, battery and DC/DC converters on energy generation side and motor controller inverters, induction motors, propellers and other loads (like hotel loads, weaponry facilities, etc) on consumption side. Within the context of this paper, the focus is on the consumption side where a set of diesel generator act as a prime-mover. The generator is connected to a six-pulse rectifier where the AC/DC conversion process is carried out. The DGR set is connected to the consumption side through a DC-link which in our study consists of a capacitor. The schematic of the system under study is shown in Figure 1.

In this study, the objective is to enhance the performance of the DGR set in terms of voltage regulation and overall system stability by introducing a novel strategy. The system outputs in this context are the DC voltage of the capacitor and the shaft speed of the diesel generator. On the other hand, the inputs of the system are the field voltage of the generator and fuel index of the diesel engine.

2.1 Diesel Engine

The diesel engine acts as the main energy producer which converts chemical energy to mechanical energy. The produced power appears as torque generation. The diesel engine dynamics can be approximated by nonlinear or linear equations (see e.g., Izadi-Zamanabadi and Blanke (1999); Grimmelius (2007)) depending on the level of accuracy needed. In this paper, a linear model is adopted to accomodate the relationship between fuel index and produced torque (Q_{en}) by means of a transfer function as below (Blanke and Andersen (1984)):

$$\dot{Q}_{\mathrm{en}} = -\frac{Q_{\mathrm{en}}}{\tau_{\mathrm{s}}} + K_{\mathrm{en}} f_{\mathrm{en}}, \tag{1}$$

where K_{en} is the torque constant, f_{en} is the governor setting (i.e., fuel index and flow) and τ_{s} is the torque buildup constant which determines the response speed of the diesel engine.

2.2 Synchronous Generator

The mechanical power is transformed to electrical power by the use of synchronous generators. The relationship between the generator and the diesel engine is established through the shaft speed where the generated torque of the diesel engine is an input for the generator. In the context of this research, the Park equivalent Direct-Quadratic (dq) modeling is used to represent the dynamics of synchronous generator. The relationship between the voltages, fluxes and currents in dq reference frame is established using the below equations:

$$\begin{aligned}
\dot{\psi}_{\mathrm{d}} &= -v_{\mathrm{d}} + \omega_{\mathrm{dg}}\psi_{\mathrm{q}} + r_{\mathrm{s}} i_{\mathrm{d}} \\
\dot{\psi}_{\mathrm{q}} &= -v_{\mathrm{q}} + \omega_{\mathrm{dg}}\psi_{\mathrm{d}} + r_{\mathrm{s}} i_{\mathrm{q}} \\
\dot{\psi}_{\mathrm{fd}} &= v_{\mathrm{fd}} - r_{\mathrm{fd}} i_{\mathrm{fd}} \\
\dot{\psi}_{\mathrm{kd}} &= -r_{\mathrm{kd}} i_{\mathrm{kd}} \\
\dot{\psi}_{\mathrm{kq}} &= -r_{\mathrm{kq}} i_{\mathrm{kq}}
\end{aligned} \tag{2}$$

where r_{s}, r_{fd}, r_{kd} and r_{kq} are per-unit stator, field circuit and damping resistances, respectively. Variables ψ_{d} and ψ_{q} are fluxes in d and q axis, ψ_{kd} and ψ_{kq} are damper fluxes and field flux is shown by ψ_{fd}. In the above model, v_{d} and v_{q} are dq voltages and v_{fd} is the field voltage of the generator. The mechanical dynamics of the synchronous generator is given as:

$$\begin{aligned}
\dot{\omega}_{\mathrm{dg}} &= \frac{1}{2H}(\psi_{\mathrm{d}} i_{\mathrm{q}} - \psi_{\mathrm{q}} i_{\mathrm{d}} + Q_{\mathrm{en}}) \\
\dot{\delta}_{\mathrm{dg}} &= \omega_{\mathrm{dg}} - 1
\end{aligned} \tag{3}$$

where ω_{dg} is the shaft speed of the diesel generator, Q_{en} is the mechanical torque produced by the diesel engine and H is the inertia constant. Variable δ_{dg} is the power angle of the generator. Using the system inductances, the relationship between electrical currents and fluxes can be established as below:

$$\begin{bmatrix} i_{\mathrm{d}} \\ i_{\mathrm{q}} \\ i_{\mathrm{fd}} \\ i_{\mathrm{kd}} \\ i_{\mathrm{kq}} \end{bmatrix} = \begin{bmatrix} x_{\mathrm{d}} & 0 & -x_{\mathrm{md}} & -x_{\mathrm{md}} & 0 \\ 0 & x_{\mathrm{q}} & 0 & 0 & -x_{\mathrm{mq}} \\ x_{\mathrm{md}} & 0 & -x_{\mathrm{fd}} & -x_{\mathrm{md}} & 0 \\ x_{\mathrm{md}} & 0 & -x_{\mathrm{md}} & -x_{\mathrm{kd}} & 0 \\ 0 & x_{\mathrm{mq}} & 0 & 0 & -x_{\mathrm{kq}} \end{bmatrix}^{-1} \begin{bmatrix} \psi_{\mathrm{d}} \\ \psi_{\mathrm{q}} \\ \psi_{\mathrm{fd}} \\ \psi_{\mathrm{kd}} \\ \psi_{\mathrm{kq}} \end{bmatrix} \tag{4}$$

where x_{d}, x_{md}, x_{kd}, x_{fd}, x_{q}, x_{mq} and x_{kq} are per unit inductances (P. C. Krause and Pekarek (2013)).

2.3 Rectifier and the DC Link

In the context of this research, an average value model with constant parameters is considered for the uncontrollable rectifier (Jatskevich et al. (2006)). In our model, the rectifier is introduced to the benchmark with generator currents as input and DC current as the output. The DC current can be computed as:

$$i_{\mathrm{dc}} = \beta_{\mathrm{rec}} \sqrt{i_{\mathrm{q}}^2 + i_{\mathrm{d}}^2}. \tag{5}$$

The DC link voltage is derived using the below Kirchhoff equation:

$$\dot{v}_{\mathrm{dc}} = \frac{1}{C}\big(i_{\mathrm{dc}} - i_{\mathrm{load}}\big) \tag{6}$$

where i_{load} is the DC load current. Moreover, the dq-voltages from the rectifier to the generator are as follows:

$$\begin{aligned} v_{\mathrm{q}} &= \alpha_{\mathrm{rec}} v_{\mathrm{dc}} \cos(\theta_{\mathrm{g}}) \\ v_{\mathrm{d}} &= \alpha_{\mathrm{rec}} v_{\mathrm{dc}} \sin(\theta_{\mathrm{g}}) \end{aligned} \tag{7}$$

where θ_g is the load angle and is computed as below:

$$\theta_{\mathrm{g}} = \arctan(\frac{i_{\mathrm{d}}}{i_{\mathrm{q}}}) - \phi_{\mathrm{rec}}. \tag{8}$$

Variables α_{rec}, β_{rec} and ϕ_{rec} are dependent on the load condition and in this model are considered to be constant.

2.4 State Space Modeling

In this part, the overall system is modeled in state space format. By rewriting (2) in matrix form:

$$\begin{bmatrix} \dot{\psi}_{\mathrm{d}} \\ \dot{\psi}_{\mathrm{q}} \\ \dot{\psi}_{\mathrm{fd}} \\ \dot{\psi}_{\mathrm{kd}} \\ \dot{\psi}_{\mathrm{kq}} \end{bmatrix} = \begin{bmatrix} 0 & -\omega_{\mathrm{dg}} & 0 & 0 & 0 \\ -\omega_{\mathrm{dg}} & 0 & 0 & 0 & 0 \\ 0 & 0 & 0 & 0 & 0 \\ 0 & 0 & 0 & 0 & 0 \\ 0 & 0 & 0 & 0 & 0 \end{bmatrix} \begin{bmatrix} \psi_{\mathrm{d}} \\ \psi_{\mathrm{q}} \\ \psi_{\mathrm{fd}} \\ \psi_{\mathrm{kd}} \\ \psi_{\mathrm{kq}} \end{bmatrix} + \begin{bmatrix} r_{\mathrm{s}} & 0 & 0 & 0 & 0 \\ 0 & r_{\mathrm{s}} & 0 & 0 & 0 \\ 0 & 0 & -r_{\mathrm{fd}} & 0 & 0 \\ 0 & 0 & 0 & -r_{\mathrm{kd}} & 0 \\ 0 & 0 & 0 & 0 & -r_{\mathrm{kq}} \end{bmatrix} \begin{bmatrix} i_{\mathrm{d}} \\ i_{\mathrm{q}} \\ i_{\mathrm{fd}} \\ i_{\mathrm{kd}} \\ i_{\mathrm{kq}} \end{bmatrix} + \begin{bmatrix} v_{\mathrm{d}} \\ v_{\mathrm{q}} \\ v_{\mathrm{fd}} \\ 0 \\ 0 \end{bmatrix}. \tag{9}$$

Then, by combining the above equation with (4) and (7), one has:

$$\begin{aligned} \dot{I}_{\mathrm{G}} =& X_{\mathrm{G}}^{-1} S_{\omega}(\omega_{\mathrm{dg}}) X_{\mathrm{G}} I_{\mathrm{G}} + X_{\mathrm{G}}^{-1} R_{\mathrm{G}} I_{\mathrm{G}} \\ &+ v_{dc} X_G^{-1} \begin{bmatrix} \alpha_{\mathrm{rec}} \sin(\arctan(\frac{i_{\mathrm{d}}}{i_{\mathrm{q}}}) - \phi_{\mathrm{rec}}) \\ \alpha_{\mathrm{rec}} \cos(\arctan(\frac{i_{\mathrm{d}}}{i_{\mathrm{q}}}) - \phi_{\mathrm{rec}}) \\ 0 \\ 0 \\ 0 \end{bmatrix} + X_G^{-1} b v_{\mathrm{fd}} \end{aligned} \tag{10}$$

where I_{G} is the vector of currents, X_{G} is the matrix of per unit inductances and R_{G} is the diagonal matrix of resistances. Moreover,

$$S_{\omega}(\omega_{\mathrm{dg}}) = \begin{bmatrix} 0 & \omega_{\mathrm{dg}} & 0 & 0 & 0 \\ \omega_{\mathrm{dg}} & 0 & 0 & 0 & 0 \\ 0 & 0 & 0 & 0 & 0 \\ 0 & 0 & 0 & 0 & 0 \\ 0 & 0 & 0 & 0 & 0 \end{bmatrix}$$

and $b = [0\ 0\ 1\ 0\ 0]^T$.

The dynamics of the diesel generator shaft speed can be represented in matrix form as below:

$$\begin{aligned} \dot{\omega}_{\mathrm{dg}} &= \frac{1}{2H}(Q_{\mathrm{en}} - I_{\mathrm{G}} X_{\mathrm{G}}^T G_1 I_{\mathrm{G}}) \\ \dot{Q}_{\mathrm{en}} &= -\frac{Q_{\mathrm{en}}}{\tau_{\mathrm{s}}} + K_{\mathrm{en}} f_{\mathrm{en}} \end{aligned} \tag{11}$$

where

$$G_1 = \begin{bmatrix} 0 & 1 & 0 & 0 & 0 \\ -1 & 0 & 0 & 0 & 0 \\ 0 & 0 & 0 & 0 & 0 \\ 0 & 0 & 0 & 0 & 0 \\ 0 & 0 & 0 & 0 & 0 \end{bmatrix}.$$

Finally, the dynamics of the DC link voltage can be written as:

$$\dot{v}_{\mathrm{dc}} = \frac{1}{C}(\beta_{\mathrm{rec}} \sqrt{I_{\mathrm{G}}^T G_2 I_{\mathrm{G}}} - i_{\mathrm{load}}) \tag{12}$$

where

$$G_2 = \begin{bmatrix} 1 & 0 & 0 & 0 & 0 \\ 0 & 1 & 0 & 0 & 0 \\ 0 & 0 & 0 & 0 & 0 \\ 0 & 0 & 0 & 0 & 0 \\ 0 & 0 & 0 & 0 & 0 \end{bmatrix}.$$

As a result, the overall dynamics of the DGR set can be described using the equations below:

$$\begin{aligned} \dot{I}_{\mathrm{G}} =& X_{\mathrm{G}}^{-1} S_{\omega}(\omega_{\mathrm{dg}}) X_{\mathrm{G}} I_{\mathrm{G}} + X_{\mathrm{G}}^{-1} R_{\mathrm{G}} I_{\mathrm{G}} \\ &+ v_{dc} X_G^{-1} \begin{bmatrix} \alpha_{\mathrm{rec}} \sin(\arctan(\frac{i_{\mathrm{d}}}{i_{\mathrm{q}}}) - \phi_{\mathrm{rec}}) \\ \alpha_{\mathrm{rec}} \cos(\arctan(\frac{i_{\mathrm{d}}}{i_{\mathrm{q}}}) - \phi_{\mathrm{rec}}) \\ 0 \\ 0 \\ 0 \end{bmatrix} + X_G^{-1} b v_{\mathrm{fd}} \\ \dot{\omega}_{\mathrm{dg}} =& \frac{1}{2H}(Q_{\mathrm{en}} - I_{\mathrm{G}} X_{\mathrm{G}}^T G_1 I_{\mathrm{G}}) \\ \dot{v}_{\mathrm{dc}} =& \frac{\beta_{\mathrm{rec}}}{C}(\sqrt{I_{\mathrm{G}}^T G_2 I_{\mathrm{G}}} - i_{\mathrm{load}}) \\ \dot{Q}_{\mathrm{en}} =& -\frac{Q_{\mathrm{en}}}{\tau_{\mathrm{s}}} + K_{\mathrm{en}} f_{\mathrm{en}} \end{aligned} \tag{13}$$

where i_{d}, i_{q}, i_{fd}, i_{kd}, i_{kq}, ω_{dg}, v_{dc} and Q_{en} are states of the system, v_{fd} and f_{en} are system inputs and ω_{dg} and v_{dc} are output variables of the system which should be controlled. Note that i_{load} appears as a disturbance to the system. The equations can be summarized in state-space format:

$$\begin{aligned} \dot{x} &= f(x) + \sum_{j=1}^{2} g_j(x) u_j + \omega \\ y_i &= h_i(x) \qquad i = 1, 2 \end{aligned} \tag{14}$$

where x is the vector of states, u is the vector of system inputs and vector y contains the system outputs. Function $f : \mathbb{R}^8 \to \mathbb{R}^8$ is the state transition function. Moreover, $g_1(x) = [X_G^{-1} b, 0, 0, 0]^T$, $g_2(x) = [0, 0, 0, K_{\mathrm{en}}]^T$, $h_1(x) = \omega_{\mathrm{dg}}$ and $h_2(x) = v_{\mathrm{dc}}$. Note that, ω contains i_{load}.

In the next section, a methodology is presented to control and stabilize this highly nonlinear system which employs feedback linearization techniques.

3. THE PROPOSED CONTROL STRATEGY

In this section, the proposed methodology for DC voltage regulation and diesel generator speed control is presented. The methodology is based on Input-Output Feedback Linearization (IOFL) of the system described in the previous section where the objective is to linearize the map between transported inputs and the system outputs. Then, by adoption of a linear control rule, the transformed system is stabilized (Henson and Seborg (1997)).

The system under study is a Multi-Input-Multi-Output (MIMO) system, with two inputs and two outputs. For IOFL, we adopt a strategy known as input-output decoupling with which the input-output responses are also decoupled. System (14) is said to be input-output feedback linearizable if the vector of relative degrees $\{r_1, r_2\}$ exists under the following conditions:

1. $L_{g_j} L_f^k h_i(x) = 0$ for all $1 \leq i, j \leq 2$ and $k < r_i - 1$ where $L_S R(x) = \frac{d}{dx} R(x) \times S$ is the Lie derivative which is the directional derivative of R with respect to S.
2. The decoupling matrix $A(x)$ should be nonsingular around the operating point of the system x_0, i.e.,

$$\det\big(A(x)\big) \neq 0 \qquad for \qquad |x - x_0| \leq 0 \tag{15}$$

where

$$A(x) = \begin{bmatrix} L_{g_1} L_f^{r_1 - 1} h_1(x) & L_{g_2} L_f^{r_1 - 1} h_1(x) \\ L_{g_1} L_f^{r_2 - 1} h_2(x) & L_{g_2} L_f^{r_2 - 1} h_2(x) \end{bmatrix}. \tag{16}$$

By applying the Lie derivative to system outputs with respect to $f(x)$ successively, the vector of relative degrees is calculated that is $\{2, 2\}$. As a result, by considering the above conditions, the decoupling matrix $A(x)$ is derived as below:

$$A(x) = \begin{bmatrix} \frac{1}{H} I_{\mathrm{G}}^T X_{\mathrm{G}}^T G_1 X_{\mathrm{G}}^{-1} b & \frac{K_{\mathrm{en}}}{2H} \\ \frac{I_{\mathrm{G}}^T G_2 X_{\mathrm{G}}^{-1} b}{C\sqrt{I_{\mathrm{G}}^T G_2 I_{\mathrm{G}}}} & 0 \end{bmatrix} \tag{17}$$

which is nonsingular around the operating point(s) of the DGR set. Please note that $\|x_0\| \neq 0$.

The states of the transformed systems are calculated using equations below:

$$\begin{aligned} \zeta_1^1 &= y_1 = h_1(x) \\ \zeta_2^1 &= \dot{y}_1 = L_{(f+g_1u_1+g_2u_2)} h_1(x) \\ \zeta_3^1 &= v_1 = L^2_{(f+g_1u_1+g_2u_2)} h_1(x) \\ \zeta_1^2 &= y_2 = h_2(x) \\ \zeta_2^2 &= \dot{y}_2 = L_{(f+g_1u_1+g_2u_2)} h_2(x) \\ \zeta_3^2 &= v_2 = L^2_{(f+g_1u_1+g_2u_2)} h_2(x) \end{aligned} \tag{18}$$

where v_1 and v_2 are the system inputs for the transported linear systems. The relationship between the original system inputs u_1 and u_2 with inputs of the transported system can be written as:

$$\begin{bmatrix} u_1 \\ u_2 \end{bmatrix} = -A^{-1}(x) \begin{bmatrix} L_f^2 y_1 \\ L_f^2 y_2 \end{bmatrix} + A^{-1}(x) \begin{bmatrix} v_1 \\ v_2 \end{bmatrix}. \tag{19}$$

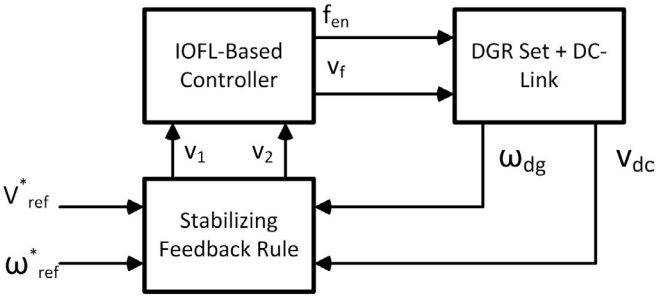

Fig. 2. Block diagram of the proposed control strategy.

The calculation results of (18) and (19) are brought in appendices. Then, the decoupled linear systems are:

$$\begin{aligned} \begin{bmatrix} \dot{\zeta}_1^1 \\ \dot{\zeta}_2^1 \end{bmatrix} &= \begin{bmatrix} 0 & 1 \\ 0 & 0 \end{bmatrix} \begin{bmatrix} \zeta_1^1 \\ \zeta_2^1 \end{bmatrix} + \begin{bmatrix} 0 \\ 1 \end{bmatrix} v_1 \\ \begin{bmatrix} \dot{\zeta}_1^2 \\ \dot{\zeta}_2^2 \end{bmatrix} &= \begin{bmatrix} 0 & 1 \\ 0 & 0 \end{bmatrix} \begin{bmatrix} \zeta_1^2 \\ \zeta_2^2 \end{bmatrix} + \begin{bmatrix} 0 \\ 1 \end{bmatrix} v_2. \end{aligned} \tag{20}$$

In order to stabilize the above systems, a stabilizing state feedback is implemented which is as follows:

$$\begin{aligned} v_1 &= -K_{11}(\zeta_1^1 - \omega_{\mathrm{ref}}) - K_{12}\zeta_2^1 \\ v_2 &= -K_{21}(\zeta_1^2 - v_{\mathrm{ref}}) - K_{22}\zeta_2^2 \end{aligned} \tag{21}$$

where ω_{ref} and v_{ref} are reference values for diesel generator shaft speed and DC voltage, respectively. Parameters K_{11}, K_{12}, K_{21} and K_{22} are state feedback controller elements. The proposed control strategy block diagram is illustrated in Figure 2.

Remark 1. Compared to conventional PI techniques for voltage regulation, the presented algorithm only requires diesel generator torque measurement and calculation of the generator currents in dq reference frame.

Remark 2. In several cases, the accurate parameters of the model are not available or unmeasured disturbances are applied to the model. Then, an integral term is required for the control of the voltage and the speed. Therefore, (21) takes the following form:

$$\begin{aligned} v_1 &= -K_{11}(\zeta_1^1 - \omega_{\mathrm{ref}}) - I_{11}\int_0^t (\zeta_1^1 - \omega_{\mathrm{ref}})d\tau - K_{12}\zeta_2^1 \\ v_2 &= -K_{21}(\zeta_1^2 - v_{\mathrm{ref}}) - I_{21}\int_0^t (\zeta_1^2 - v_{\mathrm{ref}})d\tau - K_{22}\zeta_2^2 \end{aligned} \tag{22}$$

where I_{11} and I_{21} are tuning constants associated with the integral term.

Remark 3. As shown in the previous section, the DC load current appears as a disturbance which emerges in the calculation of the transformed system states, i.e., the states of the linear transformed systems are dependent of i_{load}. The load current not only can be measured with current measurement sensors, but it also can be estimated using the efficiency curve of the induction motors and propellers (Haseltalab and Negenborn (2017)).

Remark 4. The stability of zero dynamics can be shown by the use of Lyapunov stability and invariant-set theorems which is straightforward.

In the next section, the performance of the proposed strategy is evaluated using simulations.

4. SIMULATION EXPERIMENTS

In this section, the performance of the presented algorithm is evaluated and compared to conventional PI techniques (Zahedi and Norum (2013)). Different experiments are conducted to analyze the feasibility of the proposed controller.

The simulation case in this part is a ship with 2.5 MW on-board power system and two azimuth propellers that are connected to induction motors. The induction motors are fed through the DC link by the DGR set and they can generate up to 2.2 MW propulsive power. The detailed data of the ship and power and propulsion system is brought in appendices. The Matlab Simscape toolbox is partially used for the development of the model. For Simulation, a computer with 2.8GHz Intel Core i7-7600U CPU and 8GB RAM is used.

4.1 Experiment I

We consider two experiments. In the first experiment, the ship movement is simulated in the port of Rotterdam waterways and the required power and torque for the ship movement are extracted. A short time span is chosen in which the ship takes different speeds and as a result the required power varies. The reference DC voltage is 580 V which makes the microgrid under study a low voltage DC power system. Moreover, the reference speed of the diesel generator set is $\omega_{\text{ref}} = 30$ rps which means the frequency of the power system is 60 Hz. In this experiment, it is assumed that other loads on-board of the ship absorb around 230 kW of the generated power. It is also presumed that the controllers time constants are 10 ms (for both engine governor and field voltage generator).

The simulation results are shown in Figures 3 and 4. The generated torque by one of the propellers is represented in Figure (3) where the propeller produces a varying amount of torque. The overall DC load current and generated power to meet this required power are shown as well. The shaft speed of the diesel generator is presented in per-unit which is stable and tracks the reference speed that is 1 per-unit. The DC voltage and its associated control input are shown in Figure 4 which indicates the stability of the voltage under varying loads.

4.2 Experiment II

In the second experiment, the performance of the proposed methodology is compared with the performance of conventional PI schemes where it is assumed that the DGR set is under 3000 A of load current. A line to line short circuit fault between generator and rectifier is simulated which lasts four second, between time instant $t = 4s$ and $t = 8s$. Moreover, at $t = 15s$ a sudden load drop is considered due to a failure on the consumption side of the power and propulsion system.

The results are given in Figure 5. In Figure 5a, the performance of the conventional PI schemes is compared to the performance of the proposed controller. As illustrated in this figure, the PI scheme with smaller integral constant leads to higher steady state error but can keep the system stable under these faulty situation. On the other hand,

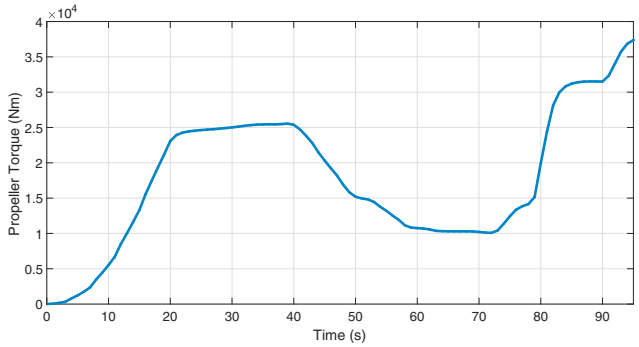

(a) Torque generated by Propeller I.

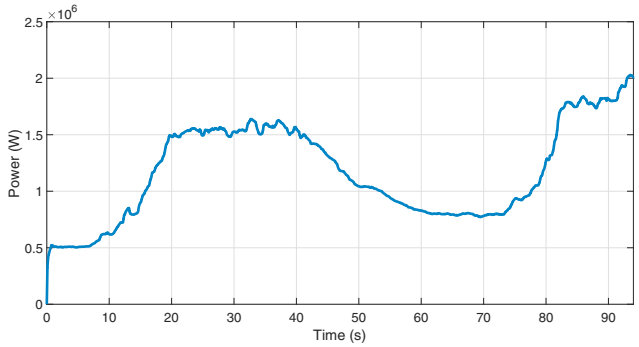

(b) Power generated by the diesel engine.

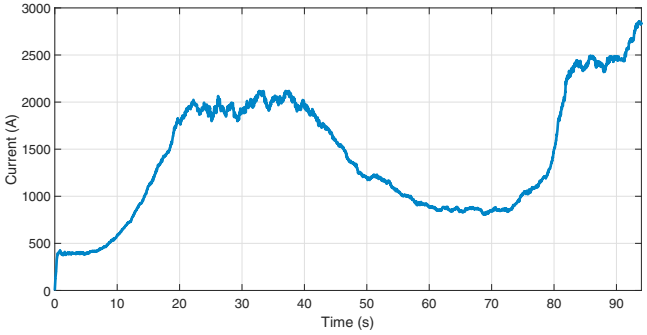

(c) Overall load current applied to the DC link.

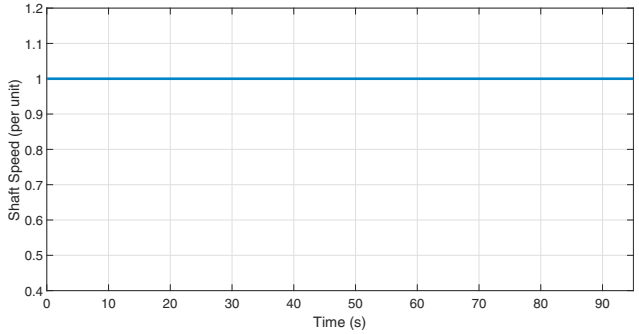

(d) Diesel generator shaft speed in per unit.

Fig. 3. Simulation results of the ship motion in port of Rotterdam waterways.

greater integral constant decreases the steady-state error but leads to instability of the system under the simulated incidents and reduces the tolerance of the system. However, by using the proposed methodology, not only the stability of the system is guaranteed but also the steady state error is very small and negligible. The diesel generator shaft speed response is shown in (5b) where the

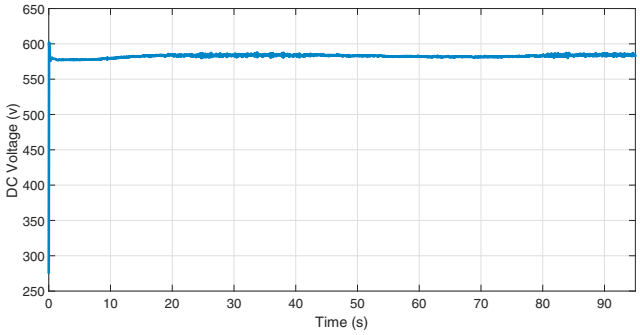

(a) DC voltage of the DC link.

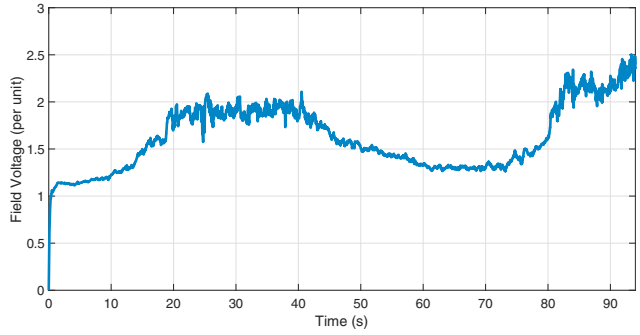

(b) Field voltage of the generator in per unit.

Fig. 4. Regulated DC voltage and field voltage of the generator for experiment I.

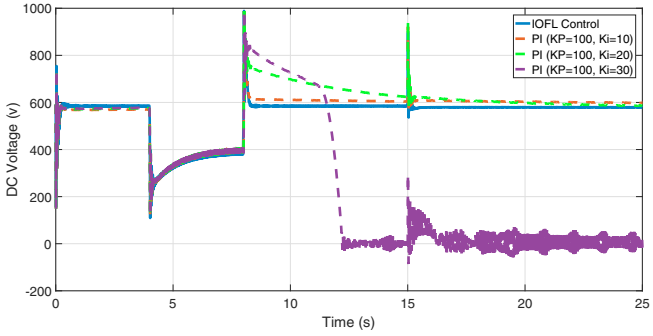

(a) Comparison of the DC voltage response.

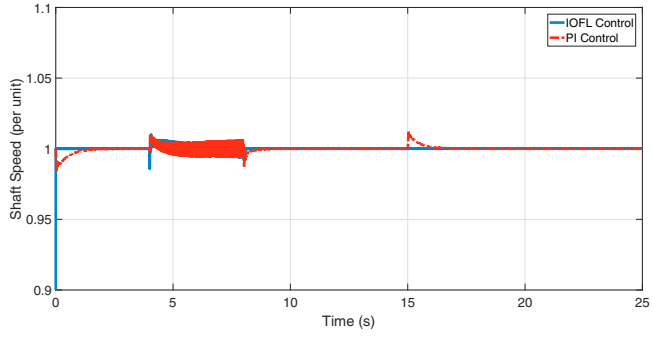

(b) Comparison of the shaft speed response.

Fig. 5. Regulated DC voltage and field voltage of the generator for experiment II.

PI controlled case is a case in which the DC voltage stays stable. The results indicate the feasibility of IOFL-based control scheme.

5. CONCLUSIONS AND FUTURE RESEARCH

In this paper, the problem of on-board DC power system stability has been considered to guarantee the DC voltage stability where a DC voltage control methodology has been proposed based on input-output feedback linearization. First, the overall system has been modeled and based on the model, the control algorithm has been designed. The simulation results show the feasibility of the proposed methodology, in terms of fault-tolerance and robustness, in comparison with conventional PI schemes.

Since, most ships have multiple prime movers on-board, an important future research direction is to extend this methodology to ships with multiple DGR sets and a set of battery-converter where distributed and cooperative schemes are employed to guarantee the stability of the power system.

ACKNOWLEDGEMENTS

Authors would like to thank the Research and Development department of Damen Shipyards Gorinchem for providing the ship model for evaluating the proposed methodology.

REFERENCES

Blanke, M. and Andersen, J. (1984). *On Dynamics of Large Two Stroke Diesel Engines: New Results from Identification.*

Farasat, M., Mehraeen, S., Arabali, A., and Trzynadlowski, A. (2015). GA-based optimal power flow for microgrids with dc distribution network. In proceedings of *IEEE Energy Conversion Congress and Exposition (ECCE)*, 3372–3379, 2015, Montreal, QC, Canada.

Geertsma, R., Negenborn, R. R., Visser, K., and Hopman, J. J. (2017). Design and control of hybrid power and propulsion systems for smart ships: A review of developments. *Applied Energy*, 194, 30 – 54.

Grimmelius, HT; Schulten, P.S.D. (2007). The use of diesel engine simulation models in ship propulsion plant design and operation. In proceedings of *CIMAC World Congress*, 1–12, 2007.

Haseltalab, A. and Negenborn, R.R. (2017). Predictive on-board power management for all-electric ships with dc distribution architecture. In proceedings of *Oceans*, 1–8, 2017, Aberdeen, Scotland.

Helland, T.H. (2015). *Stability Analysis of Diode Bridge Rectifier-Loaded Synchronous Generators Charaterized with High Values of Reactances.* Master's thesis, Norwegian University of Science and Technology.

Henson, M.A. and Seborg, D.E. (eds.) (1997). *Nonlinear Process Control.* Prentice-Hall, Inc., Upper Saddle River, NJ, USA.

Herrera, L., Zhang, W., and Wang, J. (2017). Stability analysis and controller design of dc microgrids with constant power loads. *IEEE Transactions on Smart Grid*, 8(2), 881–888.

Izadi-Zamanabadi, R. and Blanke, M. (1999). A ship propulsion system as a benchmark for fault-tolerant control. *Control Engineering Practice*, 7(2), 227 – 239.

Jatskevich, J., Pekarek, S.D., and Davoudi, A. (2006). Parametric average-value model of synchronous

machine-rectifier systems. *IEEE Transactions on Energy Conversion*, 21(1), 9–18.

Li, C., Dragicevic, T., Diaz, N.L., Vasquez, J.C., and Guerrero, J.M. (2014). Voltage scheduling droop control for state-of-charge balance of distributed energy storage in dc microgrids. In proceedings of *IEEE International Energy Conference (ENERGYCON)*, 1310–1314.

Meng, L., Shafiee, Q., Trecate, G.F., Karimi, H., Fulwani, D., Lu, X., and Guerrero, J.M. (2017). Review on control of dc microgrids and multiple microgrid clusters. *IEEE Journal of Emerging and Selected Topics in Power Electronics*, 5(3), 928–948.

Krause, P. C., O. Wasynczuk, S.D.S. and Pekarek, S. (2013). *Analysis of Electric Machinery and Drive Systems, 3rd Edition*. Wiley.

Syverud, T.H. (2016). *Modeling and Control of a DC-Grid Hybrid Power System with Battery and Variable Speed Diesel Generators*. Master's thesis, Norwegian University of Science and Technology.

Zadeh, M.K., Zahedi, B., Molinas, M., and Norum, L.E., Centralized stabilizer for marine dc microgrid. In proceedings of *39th Annual Conference of the IEEE Industrial Electronics Society*, 3359–3363, 2013, Vienna, Austria.

Zahedi, B. and Norum, L., Modeling and simulation of all-electric ships with low-voltage dc hybrid power systems. *IEEE Transactions on Power Electronics*, 28(10), 4525–4537.

Zhu, W., Shi, J., and Abdelwahed, S. (2018). End-to-end system level modeling and simulation for medium-voltage dc electric ship power systems. *International Journal of Naval Architecture and Ocean Engineering*, 10(1), 37 – 47.

Appendix A. CALCULATION RESULTS OF EQUATION (18) AND (19)

$$\begin{aligned}\zeta_1^1 =&\omega_{\rm dg}\\ \zeta_2^1 =&\frac{1}{2H}(Q_{\rm en}-I_{\rm G}X_{\rm G}^T G_1 I_{\rm G})\\ \zeta_1^2 =&v_{\rm dc}\\ \zeta_2^2 =&\frac{1}{C}(\sqrt{I_{\rm G}^T G_2 I_{\rm G}}-i_{\rm load})\end{aligned}$$

Assume,

$$E=\begin{bmatrix}\sin(\arctan(\frac{i_{\rm d}}{i_{\rm q}})-\phi_{\rm rec})\\ \cos(\arctan(\frac{i_{\rm d}}{i_{\rm q}})-\phi_{\rm rec})\\ 0\\ 0\\ 0\end{bmatrix}$$

then,

$$\begin{aligned}u_1=v_{\rm fd}=&\frac{1}{I_{\rm G}^T G_2 X_{\rm G}^{-1} b}\big(v_2-I_{\rm G}^T G_2 * X_{\rm G}^{-1} S_\omega X_{\rm G} I_{\rm G}\\ &-I_{\rm G}^T G_2 * X_{\rm G}^{-1} R_{\rm G} I_{\rm G}-v_{\rm dc} I_{\rm G}^T G_2 * X_{\rm G}^{-1} E\big)\\ u_2=f_{\rm en}=&-\frac{2}{K_{\rm en}} I_{\rm G}^T X_{\rm G} G_1 X_{\rm G}^{-1} S_\omega X_{\rm G} I_{\rm G}\\ &-\frac{2}{K_{\rm en}} I_{\rm G}^T X_{\rm G} G_1 X_{\rm G}^{-1} R_{\rm G} I_{\rm G}\\ &-\frac{2v_{\rm dc}}{K_{\rm en}} I_{\rm G}^T X_{\rm G} G_1 X_{\rm G}^{-1} E+\frac{Q_{\rm en}}{K_{\rm en}\tau_{\rm s}}+\frac{2H}{K_{\rm en}} v_1\\ &-\frac{2C}{K_{\rm en}} I_{\rm G}^T X_{\rm G} G_1 X_{\rm G}^{-1} b\frac{\sqrt{I_{\rm G}^T G_2 I_{\rm G}}}{I_{\rm G}^T X_{\rm G} G_2 X_{\rm G}^{-1} b} v_2\\ &+\frac{2}{K_{\rm en}}\frac{I_{\rm G}^T X_{\rm G} G_1 X_{\rm G}^{-1} b}{I_{\rm G}^T X_{\rm G} G_2 X_{\rm G}^{-1} b}\big(I_{\rm G}^T G_2 * X_{\rm G}^{-1} S_\omega X_{\rm G} I_{\rm G}\\ &I_{\rm G}^T G_2 * X_{\rm G}^{-1} R_{\rm G} I_{\rm G}+v_{\rm dc} I_{\rm G}^T G_2 * X_{\rm G}^{-1} E\big)\end{aligned}$$

For the design of controller, it is assumed that rectifier is ideal, i.e., $\beta_{\rm rec}=1$ and $\alpha_{\rm rec}=1$.

Appendix B. THE SHIP AND ITS POWER SYSTEM SPECIFICATIONS

- **The ship model:** Length: 90 m, deadweight at design draught: 425 tons.
- **Induction motors:** 1.1 MW, 460 v, 60 Hz, four poles.
- **Diesel Engine:** $\tau_{\rm s}=0.005$, $K_{\rm en}=1.5e6$.
- **Synchronous generator:** 2.5 MW, 460 v, 60 Hz, 4 poles, $H=0.35$, $r_s=0.009$, $r_{\rm fd}=0.002$, $r_{\rm kd}=0.3$, $r_{\rm kq}=0.025$, $x_{\rm d}=2.4$, $x_{\rm md}=2.35$, $x_{\rm kd}=3.7$, $x_{\rm fd}=0.5$, $x_{\rm q}=1.77$, $x_{\rm mq}=1.72$ and $x_{\rm kq}=0.025$. The numbers are in per-unit.
- **Rectifier:** Six-pulse rectifier, $r_{\rm sn}=10$ ohms and $C_{\rm sn}=1e-3$ F.
- **DC-link:** $C=0.05$ F.